JAERI-M
91-016

# SIMULATION ANALYSIS OF JT-60 PELLET INJECTION EXPERIMENTS

February 1991

Katsuhiro SHIMIZU, Ryuji YOSHINO
Yutaka KAMADA and Toshio HIRAYAMA

日本原子力研究所
Japan Atomic Energy Research Institute

JAERI-Mレポートは，日本原子力研究所が不定期に公刊している研究報告書です。
入手の問合わせは，日本原子力研究所技術情報部情報資料課（〒319-11 茨城県那珂郡東海村）あて，お申しこみください。なお，このほかに財団法人原子力弘済会資料センター（〒319-11 茨城県那珂郡東海村日本原子力研究所内）で複写による実費領布をおこなっております。

JAERI-M reports are issued irregularly.
Inquiries about availability of the reports should be addressed to Information Division Department of Technical Information, Japan Atomic Energy Research Institute, Tokaimura, Naka-gun, Ibaraki-ken 319-11, Japan.



編集兼発行　日本原子力研究所
印　　刷　ニッセイエブロ株式会社

JAERI-M 91-016

# Simulation Analysis of JT-60 Pellet Injection Experiments

Katsuhiro SHIMIZU, Ryuji YOSHINO
Yutaka KAMADA and Toshio HIRAYAMA

Department of Large Tokamak Research
Naka Fusion Research Establishment
Japan Atomic Energy Research Institute
Naka-machi, Naka-gun, Ibaraki-ken

(Received January 30, 1991)

The transport of pellet fuelled plasmas in JT-60 has been investigated with a predictive tokamak transport code. The inward pinch of ~0.2 m/sec at the half plasma radius and the reduced particle diffusion coefficient in the central region of 0.1 $m^2/s$ are necessary to explain the peaked density profile observed in the pellet fuelled plasma. These particle transport properties yield the improved energy confinement in the plasma with the strong particle source in the hot core region under the sawtooth suppression condition. The plasma current dependence of the improved stored energy can be explaind by the assumption that the particle confinement is good within the $q = 1$ surface.

Keywords: JT-60, Pellet, Sawtooth, Confinement, Transport, Inward Pinch, Simulation

JAERI-M 91-016

# ＪＴ－６０のペレット入射実験のシミュレーション解析

日本原子力研究所那珂研究所臨界プラズマ研究部
清水　勝宏・芳野　隆治・鎌田　　裕・平山　俊雄

（１９９１年１月30日受理）

トカマク輸送コードを用いて，ＪＴ－６０のペレット・プラズマの輸送解析を行った。ペレット入射プラズマで観測されたピークした密度分布を説明するには，内向きの粒子ピンチ（プラズマ半径の半分の位置で，0.2m/s 程度）の発生と，q＝1面内での粒子拡散係数の減少($0.1m^2/s$ 程度）が必要である。q＝1面内での良好な粒子閉じ込めは，プラズマ中心部に強い粒子供給が有り，鋸歯状振動が抑制された時，エネルギー閉じ込め改善をもたらす。それは，ペレット実験で得られたエネルギー閉じ込め改善のプラズマ電流依存性を説明する。

那珂研究所：〒311-01　茨城県那珂郡那珂町大字向山801-1

Contents

# 目　　次

# 1. Introduction

One of the methods to enhance plasma performance is to produce plasmas with a highly peaked pressure profile. Because pellet injection has the advantage of realizing such plasmas, pellet injection experiments have been carried out in many tokamaks [ 1,2,3,4 ]. The improved energy confinement has been observed in association with the improved particle confinement. In JT-60, the plasma stored energy was enhanced by about 30 ~ 40 % relative to gas fuelled plasmas at Ip = 2.8 ~ 3.1 MA plasmas with 10 ~ 15 MW NB heating [ 5,6,7 ]. The sawtooth oscillation was suppressed during 0.4 ~ 1 sec after the pellet injection for the well center fuelled pellet injection discharges. The peaked density profile was sustained during this sawtooth free phase.

One of the key issues for the fusion research is to understand the transport process and the mechanism of the improved confinement in H-mode plasma or peaked density plasmas with pellet fuelling. In ALCATOR-C, it was shown that the improvement of energy confinement in pellet fuelled plasmas was attributed to the reduced ion conduction which may be induced by the suppression of the ion temperature gradient mode due to the peaked density profile [ 8 ]. In TEXT, the reduced ion conduction was also observed after the pellet injection but was not sufficient to explain the whole improved energy confinement [ 4 ] . In such transport analysis, the heat diffusivities were inferred from the measured temperature profiles and the density profiles. But the lacking of measurements of the ion temperature in time and space limited the accuracy of the inferred heat diffusivity because of large equi-partition at the high density. In addition, it is not clear the relation between the improved energy transport and the improved particle transport. In order to understand the transient behaviors of transport linked with each other, simulation analysis where the particle and the energy balance equations are solved simultaneously is necessary. The purpose of this paper is to clarify the transport modification after the pellet injection using the predictive transport code. The effect of the sawtooth suppression on the energy confinement is also investigated.

This paper is arranged as follows : In section 2, the pellet injected experiments are described briefly. Section 3 describes the simulation model. The simulation results and

discussion are presented in section 4. The summary is presented in section 5. In Appendix A, the effect of the reduced heat diffusivity within the q = 1 surface on the electron temperature is presented. The correlation between the penetration depth and the sawtooth suppression is investigated using a new model of sawtooth and simulation results are presented in Appendix B.

## 2. Experimental Results

The energy confinement time for pellet fuelled discharges has been improved by about 30 ~ 40 % relative to gas fuelled plasma discharges in JT-60 [ 5,7 ]. Figure 1 shows the power dependence of stored energy measured by a diamagnetic loop. Open symbols and closed symbols represent the stored energies of gas fuelled plasmas and pellet fuelled plasmas, respectively. The stored energy is improved by ~ 0.5 MJ at a high plasma current with the medium heating power of 10 ~ 15 MW. The improvement increases with the plasma current and is reduced with the heating power above 15 MW. The electron pressure profile measured by Thomson data and soft X-ray data indicates that the improvement in the stored energy is mainly due to the peaked pressures profile inside the q = 1 surface [ 6 ].

In the well-center fuelled pellet injection discharges, the peaked density profile with $n_e(0) \approx 2.5 \sim 3 \times 10^{20}$ m$^{-3}$ was sustained during 0.4 ~ 1 sec after the pellet injection. Figure 2 (a) shows the time evolution of the neutral beam heating power $P_{NB}$, soft X-ray signals of central chord, the stored energy measured by diamagnetic loop and the line-integrated density at r = 0.5 a ( a is the minor radius ) for the shot E10814. Four pellets were injected at 6 sec into the NB heated plasma with $I_p = 3.1$ MA and $B_T = 4.5$ T . The beam heating power was increased from 6 MW up to 14 MW after the pellet injection. The stored energy of the pellet fuelled plasma was improved by 0.5 MJ larger than that of the gas fuelled plasma with the same heating power of 14 MW. Figure 2(b) shows the density profiles measured by Thomson scattering. The sawtooth was suppressed for nearly 1 sec after pellet injection and the peaked density profile was kept during this sawtooth free phase. The particle confinement time in the

discussion are presented in section 4. The summary is presented in section 5. In Appendix A, the effect of the reduced heat diffusivity within the q = 1 surface on the electron temperature is presented. The correlation between the penetration depth and the sawtooth suppression is investigated using a new model of sawtooth and simulation results are presented in Appendix B.

## 2. Experimental Results

The energy confinement time for pellet fuelled discharges has been improved by about 30 ~ 40 % relative to gas fuelled plasma discharges in JT-60 [ 5,7 ]. Figure 1 shows the power dependence of stored energy measured by a diamagnetic loop. Open symbols and closed symbols represent the stored energies of gas fuelled plasmas and pellet fuelled plasmas, respectively. The stored energy is improved by ~ 0.5 MJ at a high plasma current with the medium heating power of 10 ~ 15 MW. The improvement increases with the plasma current and is reduced with the heating power above 15 MW. The electron pressure profile measured by Thomson data and soft X-ray data indicates that the improvement in the stored energy is mainly due to the peaked pressures profile inside the q = 1 surface [ 6 ].

In the well-center fuelled pellet injection discharges, the peaked density profile with $n_e(0) \approx 2.5 \sim 3 \times 10^{20}$ m$^{-3}$ was sustained during 0.4 ~ 1 sec after the pellet injection. Figure 2 (a) shows the time evolution of the neutral beam heating power $P_{NB}$, soft X-ray signals of central chord, the stored energy measured by diamagnetic loop and the line-integrated density at r = 0.5 a ( a is the minor radius ) for the shot E10814. Four pellets were injected at 6 sec into the NB heated plasma with $I_p = 3.1$ MA and $B_T = 4.5$ T . The beam heating power was increased from 6 MW up to 14 MW after the pellet injection. The stored energy of the pellet fuelled plasma was improved by 0.5 MJ larger than that of the gas fuelled plasma with the same heating power of 14 MW. Figure 2(b) shows the density profiles measured by Thomson scattering. The sawtooth was suppressed for nearly 1 sec after pellet injection and the peaked density profile was kept during this sawtooth free phase. The particle confinement time in the

central region estimated from the density profiles reached 3 sec, which indicated an improved particle confinement in the central region.

In the shot of E10243, it was observed that the density profiles peaked gradually after pellet injection. The pellet injection scenario is shown in Fig. 3(a). Two pellets were injected into the neutral beam heated plasma with 8 MW. The sawtooth was suppressed for ~ 0.4 sec after pellet injection and the stored energy was improved by about 0.5 MJ relative to the gas fuelled plasma. The density profiles just after (0.02 sec) and 0.4 sec later than the pellet injection are shown in Fig. 3(b). The density in the outer region decreased after the pellet injection while the density inside the q = 1 surface increased to some extent. This density evolution suggests the particle inward pinch.

Sawtooth suppression strongly depended on the penetration length of pellet ( see Fig. 14 ). The sawtooth was suppressed during 0.4 ~ 1 sec after pellet injection when the pellet reached the central region of the plasma along the pellet injection path. The improvement of the stored energy increased with the peaking factor of density ( see Fig. 16 ).

## 3. Simulation model

Simulations have been performed with the 1-1/2 dimensional transport code including the following model.

### 3.1 Pellet Ablation Model

The ablation profile of the pellet is calculated by the neutral-gas shielding model [ 9 ]. Fast ions have strong effect on the ablation profiles. The particle density of fast ions is calculated from the Stix's steady state solution [ 10 ], in which the charge exchange loss is not included. The Orbit-Following Monte-Carlo code ( OFMC code ) [ 11 ] including the orbit effect and the charge exchange loss shows that the fast ion density in the plasma peripheral region is

central region estimated from the density profiles reached 3 sec, which indicated an improved particle confinement in the central region.

In the shot of E10243, it was observed that the density profiles peaked gradually after pellet injection. The pellet injection scenario is shown in Fig. 3(a). Two pellets were injected into the neutral beam heated plasma with 8 MW. The sawtooth was suppressed for ~ 0.4 sec after pellet injection and the stored energy was improved by about 0.5 MJ relative to the gas fuelled plasma. The density profiles just after (0.02 sec) and 0.4 sec later than the pellet injection are shown in Fig. 3(b). The density in the outer region decreased after the pellet injection while the density inside the q = 1 surface increased to some extent. This density evolution suggests the particle inward pinch.

Sawtooth suppression strongly depended on the penetration length of pellet ( see Fig. 14 ). The sawtooth was suppressed during 0.4 ~ 1 sec after pellet injection when the pellet reached the central region of the plasma along the pellet injection path. The improvement of the stored energy increased with the peaking factor of density ( see Fig. 16 ).

## 3. Simulation model

Simulations have been performed with the 1-1/2 dimensional transport code including the following model.

### 3.1 Pellet Ablation Model

The ablation profile of the pellet is calculated by the neutral-gas shielding model [ 9 ]. Fast ions have strong effect on the ablation profiles. The particle density of fast ions is calculated from the Stix's steady state solution [ 10 ], in which the charge exchange loss is not included. The Orbit-Following Monte-Carlo code ( OFMC code ) [ 11 ] including the orbit effect and the charge exchange loss shows that the fast ion density in the plasma peripheral region is

extremely reduced. Therefore, the fast ion effect on the pellet ablation is reduced so as to agree with the observed penetration depth by enhancing the charge exchange loss of fast ions.

### 3.2 Sawtooth Model

We adopt a simple model for the sawtooth oscillation. In this model, the minor disruption occurs repeatedly with a fixed period $\tau_{SW}$ ( i.e. 60 msec for OH plasma, 90 msec for NB heated plasma ). After the pellet injection, the time when the sawtooth crash takes place is determined from the experimental data. When the minor disruption occurs, the profiles of the density, the electron and ion temperature and the plasma current density within the region $0 \leq r \leq r_0$ are mixed based on the conservational laws of particle, energy and magnetic flux, respectively [ 12 ]. The mixing radius $r_0$ is assumed to be $\sim 1.2\, r_s = 1.2\, a / q(a)$ , where $r_s$ is the minor radius of the q = 1 singular surface and the q(a) is the safety factor at the plasma surface.

### 3.3 Inward Pinch

Since the gas-fuelled plasma in JT-60 has a flat density profile with the typical density peaking factor $n_{e0} / \langle n_e \rangle$ of $\sim$ 1.5 in the high density regime above $\bar{n}_e = 6 \times 10^{19}$ m$^{-3}$ , no experimental data can be indicated as for the particle pinch effect obviously. On the other hand, the peaked density profile is sustained after the pellet injection during the sawtooth free phase. In addition, it has been observed that the density profile peaked after pellet injection ( see Fig. 2 (b) and Fig. 3 (b) ). Therefore, it can be considered that the inward pinch is induced after the pellet injection. For simplicity, the pinch velocity is assumed to be proportional to the minor radius,

$$V_{in}(r) = V_a\, r / a \,.$$

The pellet-fuelled plasma with the sawtooth oscillation goes back to the L-mode plasma which has no inward pinch. The inward pinch velocity is set to zero after the first sawtooth crash.

### 3.4 Diffusion Coefficients

The steady state transport analysis [ 13 ] shows that the effective heat diffusivity $\chi_{eff}$ in NB heated plasmas increases with q(r) [ 14 ]. The $\chi_{eff}$ has no density dependence in the high density regime ( $\bar{n}_e \geq 4 \times 10^{19}$ m$^{-3}$ ). Taking this analytical result into consideration, the parameter survey of the diffusion coefficient has been carried out extensively. The power degradation of the energy confinement and the improvement of the stored energy with the plasma current in the high density regime can be well reproduced by the simulation with the following diffusion coefficients.

$$D_e(r) = ( 0.2 + 0.015\, P_{NB} ) \times q(r) \quad ( m^2/s ) ,$$

$$\chi_e(r) = ( \chi_e^{OH} + 0.045\, P_{NB} ) \times q(r) \quad ( m^2/s ) ,$$

$$\chi_i(r) = \chi_i^{CH} + \chi_e ,$$

where $P_{NB}$ is the Neutral Beam power absorbed by bulk plasma in MW unit. The diffusion coefficients consist of two parts : power degradation and q-dependence parts. The peaked density profile in the pellet fuelled plasma suggests the good particle confinement in the central region [ 6 ]. It is possible to sustain the peaked density profile by the following diffusion coefficient within the q = 1 surface,

$$D_e(r) = 0.1 \ ( m^2/s ) \qquad ( q(r) \leq 1 ) .$$

The ion thermal diffusivity $\chi_i$ is assumed to be the sum of the electron thermal diffusivity, $\chi_e$ and the neoclassical diffusivity derived by Chang-Hinton, $\chi_i^{CH}$ [ 15 ]. Our simulation results are not so sensitive to this assumption because the energy equipartition between electrons and ions dominates the energy transport of in high density plasma.

The value of $\chi_e^{OH}$ is chosen so as to agree with the stored energy for Ohmic heating plasma, as following;

$\chi_e^{OH}$ ( 2.1 MA ) = 0.33 $m^2/s$ ,

$\chi_e^{OH}$ ( 3.1 MA ) = 0.24 $m^2/s$ .

Figure 4(a) shows the plasma stored energy as a function of the absorbed power for 3.1 MA ( closed diamonds ) and 2.1 MA ( closed circles ) plasmas with Bt = 4.8 T. The line-averaged density $\bar{n}_e$ are fixed at the value of $5.7 \times 10^{19}$ $m^{-3}$. The simulation results reproduce well the off-set linear characteristics of the stored energy and their values are in good agreement with the experimental data shown by the solid lines. The typical diffusion coefficients for the 3.1 MA plasma with 14 MW neutral beam heating are shown in Fig. 4 (b). The diffusion coefficient in the central region is reduced by a factor of 3 compared with that in the outer region. The calculated density and the electron temperature profiles also agree with the experimental data within the error bars. Even if the particle confinement within the q = 1 surface is improved in the gas-fuelled plasma , the density and the temperature profiles are not affected significantly. Because there is no strong particle source in the central region and the sawtooth activity flattens the density and the temperature profiles with $\tau_{sw}$ of 50 ~ 100 msec. This sawtooth period is somewhat shorter than the energy confinement time of the L-mode plasma, typically 100 ~ 200 msec.

Usually, the heat diffusivity which is taken to be proportional to the particle diffusivity ( i.e. $\chi_e = ( 1 \sim 5 ) \times D_e$ ) is employed in the predictive transport code. We have examined whether the heat diffusivity has the spatial dependence like the particle diffusion coefficient. The good energy confinement within the q = 1 surface makes the electron temperature profile peaked and the change of the central electron temperature before and after the sawtooth crash is too large compared with the experimental data. The detail is presented in Appendix A.

## 4. Simulation Results and Discussion

### 4.1 Effect of Sawtooth Activity on Plasma Stored Energy

The simulation analysis has been carried out for the shot E10814 in which the sawtooth was suppressed for nearly 1 sec after pellet injection and the peaked density profile was kept during this sawtooth free phase. Figure 5 (a) shows the ablation profiles and the density evolution obtained by the simulation. The fourth pellet reaches the closest point to the plasma center along the pellet path and the electron density at the plasma center is increased above $2.6 \times 10^{20}$ $m^{-3}$. The density decreases gradually in time and the profile happen to be flattened suddenly by the sawtooth crash at 7.0 sec. Figure 5 (b) shows the comparison of the electron temperature profiles between simulation results (solid lines) and the experimental data measured by Soft-Xray Filter Absorption method (broken lines) [16]. The electron temperature is adiabatically evolved just after the pellet injection. Therefore, the good agreement in electron temperature indicates that the ablation profiles are reasonable. Figure 6 (a) shows the calculated profiles of the electron density and the electron temperature. For comparison, the experimental data ( Thomson data ) are also plotted in this figure. The simulation results are in good agreement with the measurement within the error bars. The time evolution of the stored energy ( $W_{ST}$ ), the line-integrated density ( $\int n_e \, dl$ ) at r = 0.5 a and the electron temperature at the plasma center ( $T_{e0}$ ) are shown in Fig. 6 (b). They also agrees with the experimental data shown by the dotted lines. The comparison of $T_{e0}$ with the measurement by Electron Cyclotron Emission shows that the recovery of the central electron temperature is well reproduced by the simulation model with the same transport coefficient of the L-mode plasma, except for the inward pinch which is assumed to be induced after the pellet injection. Therefore, it can be concluded that the thermal diffusivity is not improved after the pellet injection. The decay in the stored energy after 7 sec is fast in contrast to the diamagnetic data. The analysis of soft X-ray signals shows that small amount of the central kinetic energy is released after a sawtooth crash and the sawtooth is not full reconnecting type [ 6,7 ]. The disagreement in the temporal behavior of the stored energy is due to the difference between the

full reconnecting type of sawtooth in the simulation model and the partial reconnecting type observed in the experiment.

In order to investigate the effect of the sawtooth suppression on the plasma stored energy, the simulations have been carried out with different particle diffusion coefficients within the q = 1 surface. In the case of Fig. 7 (a) the coefficient of $D_e$ ( $q(r) < 1$ ) is reduced to 0.1 $m^2/s$, while in the case of Fig. 7 (b) $D_e$ ( $q(r) < 1$ ) is proportional to the safety factor in the same way of the outside of q = 1 surface. Solid lines represent the calculation results in which the sawtooth is suppressed till 7 sec and broken lines represent those including the sawtooth with $\tau_{sw}$ = 90 msec. Figure 7 (a) shows that the difference of the stored energy between plasmas with and without sawtooth activity amounts to 0.4 MJ if the good particle confinement in the central region is assumed. However, without the good particle confinement in the central region, the suppression of the sawtooth activity makes no difference in the maximum stored energy , as shown in Fig. 7 (b). The stored energy for the gas fuelled plasma, in which the successive sawtooth crashes take place with $\tau_{sw}$ = 90 msec and there is no inward particle pinch, is shown in Fig. 7 (c). The difference of the stored energy between the pellet fuelled plasma and the gas fuelled plasma is 0.5 MJ ( = 2.97 MJ - 2.47 MJ ). This improvement is consistent with the experimental data.

### 4.2 Inward Pinch

In this subsection, the simulation result for the shot E10243 in which the density profile became more peaked after the pellet injection is described. Figure 8 (a) shows the density profiles and the electron temperature profiles. Figure 8 (b) shows that the time evolution of the stored energy and the line-integrated density at r = 0.5 a. They agree with the experimental data. In this calculation, the pinch velocity at the plasma edge $V_a$ is taken to be 0.5 m/s . The simulation result without the inward pinch, where the particle diffusion coefficient $D_e$ within the q = 1 surface is reduced to 0.03 $m^2/s$ instead of the particle pinch, is shown by the dotted line. The density profile can not be explained without the inward pinch and the improvement in the stored energy is too small compared with the diamagnetic data. There is a neoclassical

effect for particle pinch, that is, Ware pinch [ 17 ]. This pinch velocity is about 0.04 ~ 0.05 m/s, which is smaller than the inward pinch used in our simulations at the half plasma radius by a factor of 4 ~ 5.

We have examined whether the inward pinch is induced in the gas-fuelled plasma at the high density. Figure 9 (a) and (b) show the calculated density profiles excluding and including the inward pinch of $V_a$ = 0.4 m/s, respectively. The solid and dotted lines show the density profile before and after the sawtooth crash, respectively. The pinch effect is not so large because the sawtooth crash flattens the density profile with $\tau_{SW}$ = 90 msec, as shown in Fig. 9 (b). However, the inward pinch makes the density profile steep compared with the experimental data ( dash-dotted lines ). It can be concluded that there is no inward pinch in the gas-fuelled plasma, at least high density regime.

### 4.3 Power Dependence of Plasma Stored Energy

The incremental stored energy in pellet fuelled plasmas have been studied. The well center peaked ablation profiles are used for these calculations. And the sawtooth is assumed to be suppressed for 1 sec after pellet injection. Figure 10 shows the power dependence of the stored energy. The open and closed symbols represent the stored energy for the gas and pellet fuelled plasmas, respectively. The solid lines represent the stored energy including the beam component and the broken lines represent the thermal stored energy. The improvement of the thermal stored energy for 3.1 MA plasmas does not depend on the heating power and is nearly constant at the value of 0.54 MJ. On the other hand, the beam stored energy in the pellet-fuelled plasma decreases compared with that of the gas fuelled plasma due to the short slowing down time, because of the high density and the lower electron temperature. The reduction in the beam stored energy becomes significant at the high heating power and the improvement of the stored energy deteriorates in this region. As the plasma current decreases, the region of good particle confinement i.e. the radius of q =1 surface becomes narrower. As a result, the improvement of the thermal stored energy for 2.1 MA plasmas is reduced to 0.33 MJ. In Fig. 11, these simulation results ( solid and broken lines for gas and pellet fuelled plasmas,

respectively ) are compared with the experimental data ( diamonds and circles for 3.1 MA and 2.1 MA plasmas, respectively ). The power dependence and the plasma current dependence of the improved stored energy can be explained by the good particle confinement within the q = 1 surface. The sawtooth suppression during ~ 1 sec could not be obtained in low Ip discharge at the high heating power above 15 MW. This is the reason of the disagreement in this regime.

Figure 12 shows the pressure profile for 3.1 MA plasma with NBI heating power of 21 MW. The peaked pressure profile inside the q = 1 surface is obtained for pellet fuelled plasmas ( solid line ) and it is consistent with the data of soft X-ray signals [ 6 ]. The thermal stored energy within the q = 1 surface increases by 0.5 MJ compared with the gas-fuelled plasma ( broken line ). It should be noted that the peaked pressure profile is not due to the improvement in the heat diffusivity, but due to the good particle confinement within the q = 1 surface. The dot-broken line represents the pressure profile of the pellet fuelled plasma without the inward pinch. The reduction of the convection loss by the inward pinch increases the stored energy by about 0.2 MJ.

### 4.4 Relation between Penetration Depth and Improvement in Plasma Stored Energy

The center-peaked ablation profiles are used for the calculations so far. In this subsection, we have studied the relation between the penetration depth of the pellet and the improvement in the stored energy. The ablation profiles used in simulations are shown in Fig. 13 (a). The origin of the $\ell$-coordinate axes is taken to be the nearest point to the plasma center along the pellet path injection. The density profiles just after the pellet injection changes according to these ablations, as shown in Fig. 13 (b). The sawtooth start time after the pellet injection is determined from the relation based on the experimental data, as shown by solid line in Fig. 14. For example, when the penetration depth reaches to 0.2 m, the sawtooth reappears from 0.75 sec after the pellet injection. The time evolution of the stored energy are shown in Fig. 15 (a) and the density profiles at 0.5 sec after pellet injection are shown in Fig. 15 (b). The sawtooth

start time for each case are indicated by the arrows. In these simulations, the particle inward pinch is terminated after the first sawtooth crash. The stored energy starts to decrease after the sawtooth crash. The relation between the density peaking factor and the maximum stored energy is shown in Fig. 16. In order to avoid the fitting error in the experimental data, the peaking factor of the density is defined by the ratio of the density at r = 0.2 m, which is the inmost measurable position of the Thomson scattering system, and the off-axial line averaged density. Open symbols represent the simulation results. The improvement in the stored energy increases with the density peaking factor. This relation agrees well with the experimental data.

We have examined whether the inward pinch exists in the pellet fuelled plasma after a sawtooth crash. When the inward pinch is not terminated after the sawtooth crash, the simulation result is obtained as shown in Fig. 17. For the case of c or d, the stored energy continues to increase gradually after the sawtooth crash by the effect of the inward pinch. And the high density at the plasma center is sustained in spite of the sawtooth activity. This feature contradicts the experimental fact. Therefore, it can be considered that the inward pinch does not exist after a sawtooth crash any longer.

## 5. Conclusions

The transport modification after pellet injection has been investigated by using the predictive transport code with an empirical diffusion coefficient. Conclusions of the present work are as follows:

(1) The peaked density profile can be explained by the reduced particle diffusion of 0.1 $m^2/s$ in the central region and the inward particle pinch induced after the pellet injection. The pinch velocity is about 0.2 m/s at a half plasma radius.

(2) The above particle transport properties have little effect on the electron density profile in the L-mode plasma with the sawtooth activity. The good particle confinement in the central region has become noticeable by the sawtooth suppression during long time of ~ 1 sec.

start time for each case are indicated by the arrows. In these simulations, the particle inward pinch is terminated after the first sawtooth crash. The stored energy starts to decrease after the sawtooth crash. The relation between the density peaking factor and the maximum stored energy is shown in Fig. 16. In order to avoid the fitting error in the experimental data, the peaking factor of the density is defined by the ratio of the density at r = 0.2 m, which is the inmost measurable position of the Thomson scattering system, and the off-axial line averaged density. Open symbols represent the simulation results. The improvement in the stored energy increases with the density peaking factor. This relation agrees well with the experimental data.

We have examined whether the inward pinch exists in the pellet fuelled plasma after a sawtooth crash. When the inward pinch is not terminated after the sawtooth crash, the simulation result is obtained as shown in Fig. 17. For the case of c or d, the stored energy continues to increase gradually after the sawtooth crash by the effect of the inward pinch. And the high density at the plasma center is sustained in spite of the sawtooth activity. This feature contradicts the experimental fact. Therefore, it can be considered that the inward pinch does not exist after a sawtooth crash any longer.

## 5. Conclusions

The transport modification after pellet injection has been investigated by using the predictive transport code with an empirical diffusion coefficient. Conclusions of the present work are as follows:

(1) The peaked density profile can be explained by the reduced particle diffusion of 0.1 $m^2/s$ in the central region and the inward particle pinch induced after the pellet injection. The pinch velocity is about 0.2 m/s at a half plasma radius.

(2) The above particle transport properties have little effect on the electron density profile in the L-mode plasma with the sawtooth activity. The good particle confinement in the central region has become noticeable by the sawtooth suppression during long time of ~ 1 sec.

(3) The relaxation of electron temperature profile after pellet injection can be well reproduced with the diffusion coefficients of L-mode plasmas. It is indicated in these simulations that the thermal diffusivity is not improved in the pellet fuelled plasma. The reduced convection loss by the inward pinch contributes to the increase of the stored energy.

(4) Without the good particle confinement in the central region, the sawtooth suppression cannot improve the energy confinement . The plasma current dependence of the improved stored energy can be explained by the reduced particle diffusion model within the $q = 1$ surface.

## Acknowledgments

The authors would like to thank Drs. M. Azumi, K. Tani and H. Kishimoto for their fruitful discussion. They would like to express their appreciation to Drs. M. Yoshikawa, T. Iijima and S. Tamura for their encouragements and support on this work.

## References

[1] The JET Team presented by SCHMIDT, G.L., in Plasma Physics and Controlled Nuclear Fusion Research 1988 ( Proc. 12 th Int. Conf. Nice, 1988 ), Vol. 1, IAEA Vienna (1988) 215.

[2] SCHMIDT, G.L., MILORA, S.L., ARUNASALAM, V., et al., in Plasma Physics and Controlled Nuclear Fusion Research 1986 ( Proc. 11 th Int. Conf. Kyoto, 1986 ), Vol. 1, IAEA Vienna (1987) 171.

(3) The relaxation of electron temperature profile after pellet injection can be well reproduced with the diffusion coefficients of L-mode plasmas. It is indicated in these simulations that the thermal diffusivity is not improved in the pellet fuelled plasma. The reduced convection loss by the inward pinch contributes to the increase of the stored energy.

(4) Without the good particle confinement in the central region, the sawtooth suppression cannot improve the energy confinement . The plasma current dependence of the improved stored energy can be explained by the reduced particle diffusion model within the $q = 1$ surface.

## Acknowledgments

The authors would like to thank Drs. M. Azumi, K. Tani and H. Kishimoto for their fruitful discussion. They would like to express their appreciation to Drs. M. Yoshikawa, T. Iijima and S. Tamura for their encouragements and support on this work.

## References

[1] The JET Team presented by SCHMIDT, G.L., in Plasma Physics and Controlled Nuclear Fusion Research 1988 ( Proc. 12 th Int. Conf. Nice, 1988 ), Vol. 1, IAEA Vienna (1988) 215.

[2] SCHMIDT, G.L., MILORA, S.L., ARUNASALAM, V., et al., in Plasma Physics and Controlled Nuclear Fusion Research 1986 ( Proc. 11 th Int. Conf. Kyoto, 1986 ), Vol. 1, IAEA Vienna (1987) 171.

(3) The relaxation of electron temperature profile after pellet injection can be well reproduced with the diffusion coefficients of L-mode plasmas. It is indicated in these simulations that the thermal diffusivity is not improved in the pellet fuelled plasma. The reduced convection loss by the inward pinch contributes to the increase of the stored energy.

(4) Without the good particle confinement in the central region, the sawtooth suppression cannot improve the energy confinement . The plasma current dependence of the improved stored energy can be explained by the reduced particle diffusion model within the $q = 1$ surface.

## Acknowledgments

The authors would like to thank Drs. M. Azumi, K. Tani and H. Kishimoto for their fruitful discussion. They would like to express their appreciation to Drs. M. Yoshikawa, T. Iijima and S. Tamura for their encouragements and support on this work.

## References

[1] The JET Team presented by SCHMIDT, G.L., in Plasma Physics and Controlled Nuclear Fusion Research 1988 ( Proc. 12 th Int. Conf. Nice, 1988 ), Vol. 1, IAEA Vienna (1988) 215.

[2] SCHMIDT, G.L., MILORA, S.L., ARUNASALAM, V., et al., in Plasma Physics and Controlled Nuclear Fusion Research 1986 ( Proc. 11 th Int. Conf. Kyoto, 1986 ), Vol. 1, IAEA Vienna (1987) 171.

[3] KAUFMANN, M., BEHRINGER, K., FUSSMANN, G., GRUBER, O., LACKNER, K., et al., in Plasma Physics and Controlled Nuclear Fusion Research 1988 ( Proc. 12 th Int. Conf. Nice, 1988 ), Vol. 1, IAEA Vienna (1989) 229.

[4] ROWAN, W.L., BRAVENEC, R.V., WILEY, J.C., BENGTSON, R.D., DURST, R.D., et al., Nucl. Fusion **30** (1990) 903.

[5] KAMADA, Y., YOSHINO, R., NAGAMI, M., et al., Nucl. Fusion **29** (1989) 1785.

[6] KAMADA, Y., YOSHINO, R., NAGAMI, M. and OZEKI, T., submitted to Nucl. Fusion.

[7] KAMADA, Y., YOSHINO, R., NAGAMI, M., OZEKI, T., SHIMIZU, K., et al., IAEA CN 53 / A-4-3, IAEA Conference on Plasma Physics and Controlled Nuclear Fusion Research, Washington (1990).

[8] WOLFE, S.M., GREENWALD, M., GANDY, R., et al., Nucl. Fusion **26** (1986) 329.

[9] MILORA, S.L., ORNL/TM-8616 (1983).

[10] STIX, T. H., Plasma Physics **14** (1972) 367.

[11] TANI, K., AZUMI, M., Ohtsuka, M., KISHIMOTO, H., TAMURA, S., in Heating in Toroidal Plasma ( Proc. Joint Varenna Grenobel Int. Symp. 1978), Vol 1 (1978) 31.

[12] KADOMTEV, B.B., Fizika Plazmy **1** (1975) 710.

[13] HIRAYAMA, T., SHIMIZU, K., TANI, K., SHIRAI, H., KIKUCHI, M., Experimental Transport Analysis Code System in JT-60, Rep. JAERI-M90-066, Japan Atomic Energy Research Institute (1988).

[14] JT-60 Team, Review of JT-60 Experimental Results from January to October 1989, Rep. JAERI-M90-066, Japan Atomic Energy Research Institute (1990).

[15] CHANG, C.S. and HINTON, F.L., Phys. Fluids **29** (1987) 3314.

[16] NAGASHIMA, K., NISHITANI, T. and TAKEUCHI, H., Electron Temperature Profile Measurement using the Filter Absorption Method in JT-60, Rep. JAERI-M89-226, Japan Atomic Energy Research Institute (1990).

[17] WARE, A.A., Phys. Rev. Lett. **25** (1970) 15.

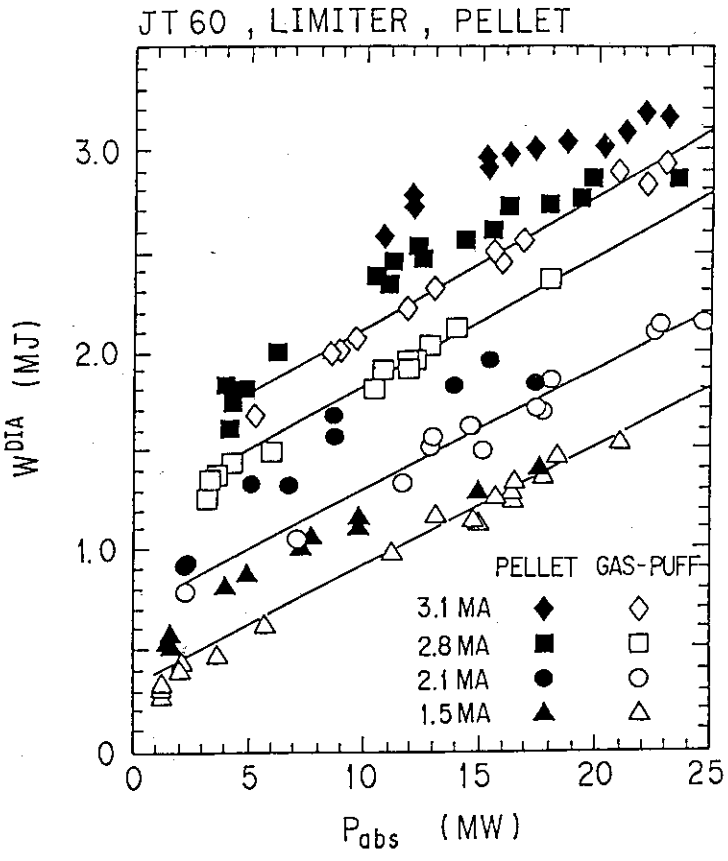


Fig. 1 Stored energy ( $W^{DIA}$ ) measured by a diamagnetic loop as a function of absorbed power ( $P_{abs}$ ) for gas-fuelled plasma ( open symbols ) and pellet fuelled plasmas ( closed symbols ).

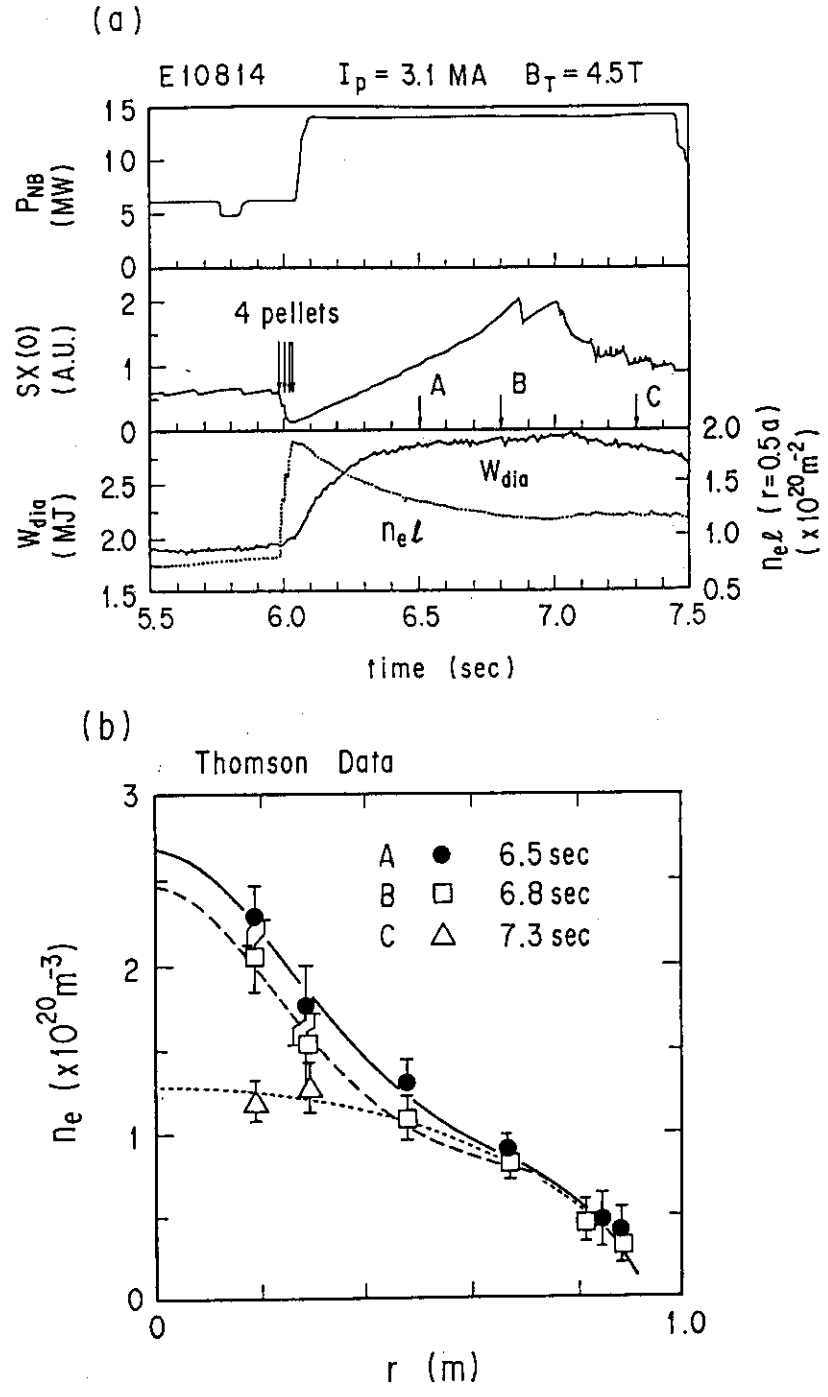


Fig. 2 (a) Pellet injection scenario for the shot E10814 with $I_p$ = 3.1 MA and $B_t$ = 4.5 T Time evolution of the beam heating power ( $P_{NB}$ ) , soft X-ray intensity of central chord ( SX(0) ), the stored energy ( $W_{dia}$ ) measured by a diamagnetic loop and the line-integrated density ( $\int n_e\, dl$ ) at r = 0.5 a.

(b) Electron density profiles obtained by Thomson measurement at three times indicated by arrows in Fig. 2 (a). The peaked density profile is kept during the sawtooth free phase.

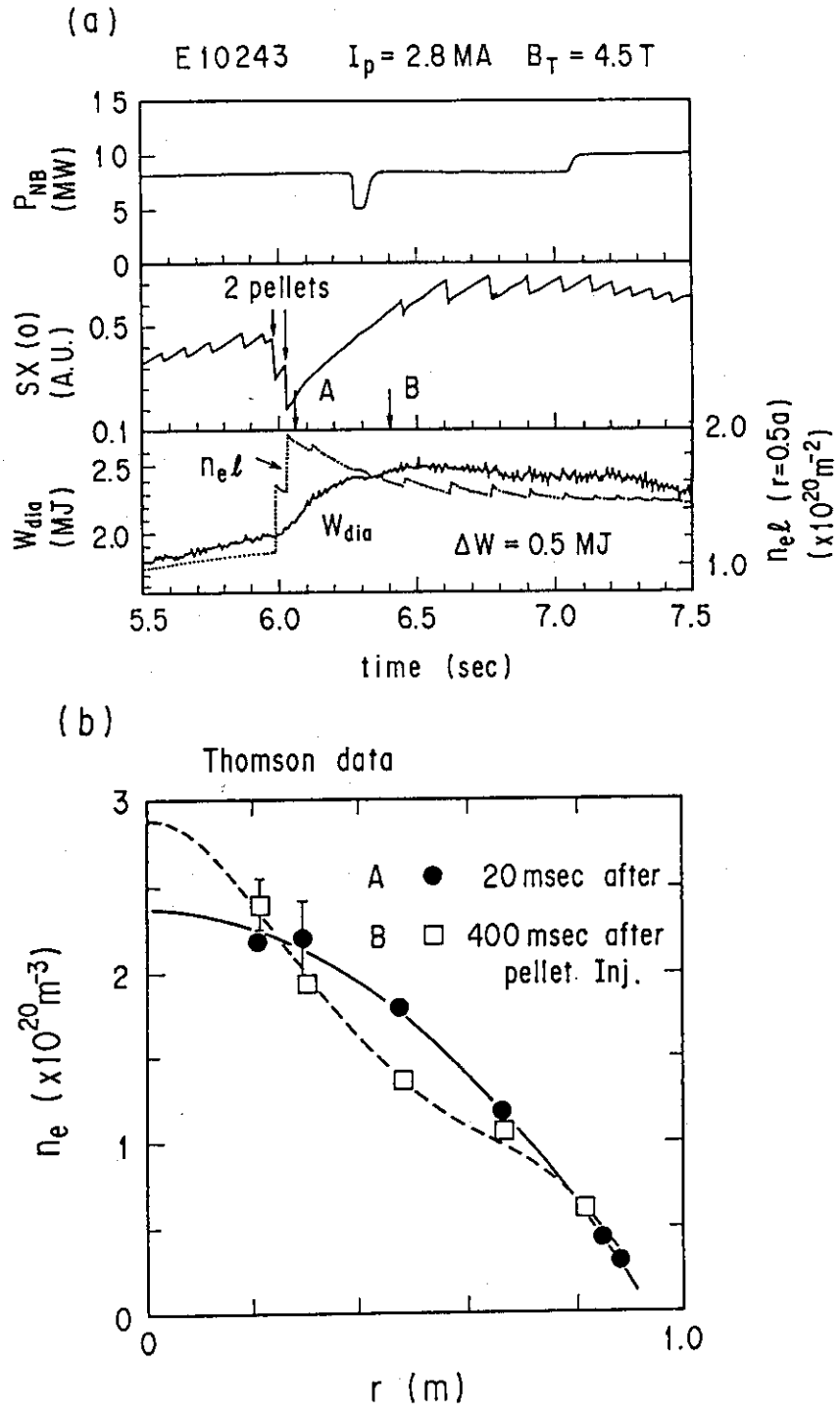


Fig. 3 (a) Pellet injection scenario for the shot E10243 with $I_p = 2.8$ MA and $B_t = 4.5$ T . Time evolution of the beam heating power ( $P_{NB}$ ) , soft X-ray intensity of central chord ( SX(0) ), the stored energy ( $W_{dia}$ ) measured by a diamagnetic loop and the line-integrated density ( $\int n_e\, dl$ ) at r = 0.5 a.

(b) Electron density profiles obtained by Thomson measurement at two times indicated by arrows in Fig. 3 (a). The density profiles peaks gradually compared with that just after ( 20 msec ) pellet injection.

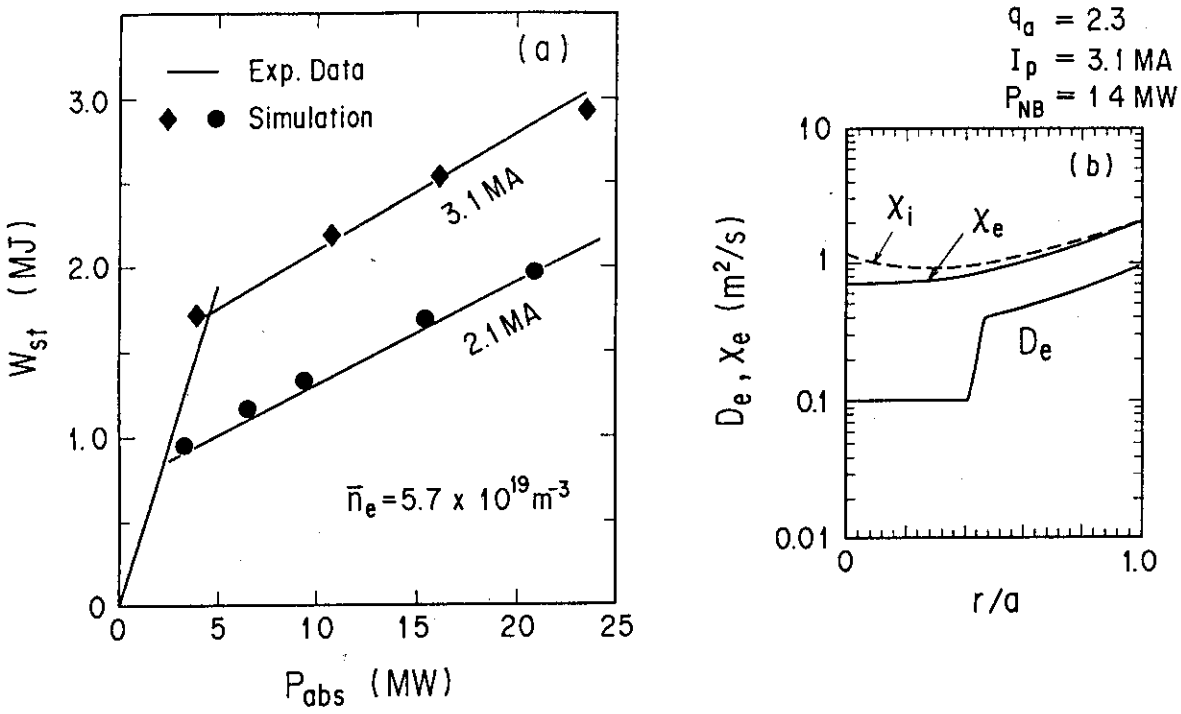


Fig. 4 (a) Relation between the plasma stored energy ( $W_{ST}$ ) obtained in simulations and the absorbed power ( $P_{abs}$ ) for 3.1 MA ( closed diamonds ) and 2.1 MA ( closed circles ) plasmas with $B_T = 4.5$ T and $\bar{n}_e = 5.7 \times 10^{19}$ $m^{-3}$. The simulation results are in good agreement with the experimental data ( solid lines ).

(b) Typical profile of diffusion coefficients for 3.1 MA plasma ( $q_a = 2.3$ ) with 14 MW beam heating power. The particle diffusion coefficient ( $D_e$ ) inside the $q = 1$ surface ( $r_s = a / q_a = 0.4\ a$ ) is reduced to 0.1 $m^2/s$ .

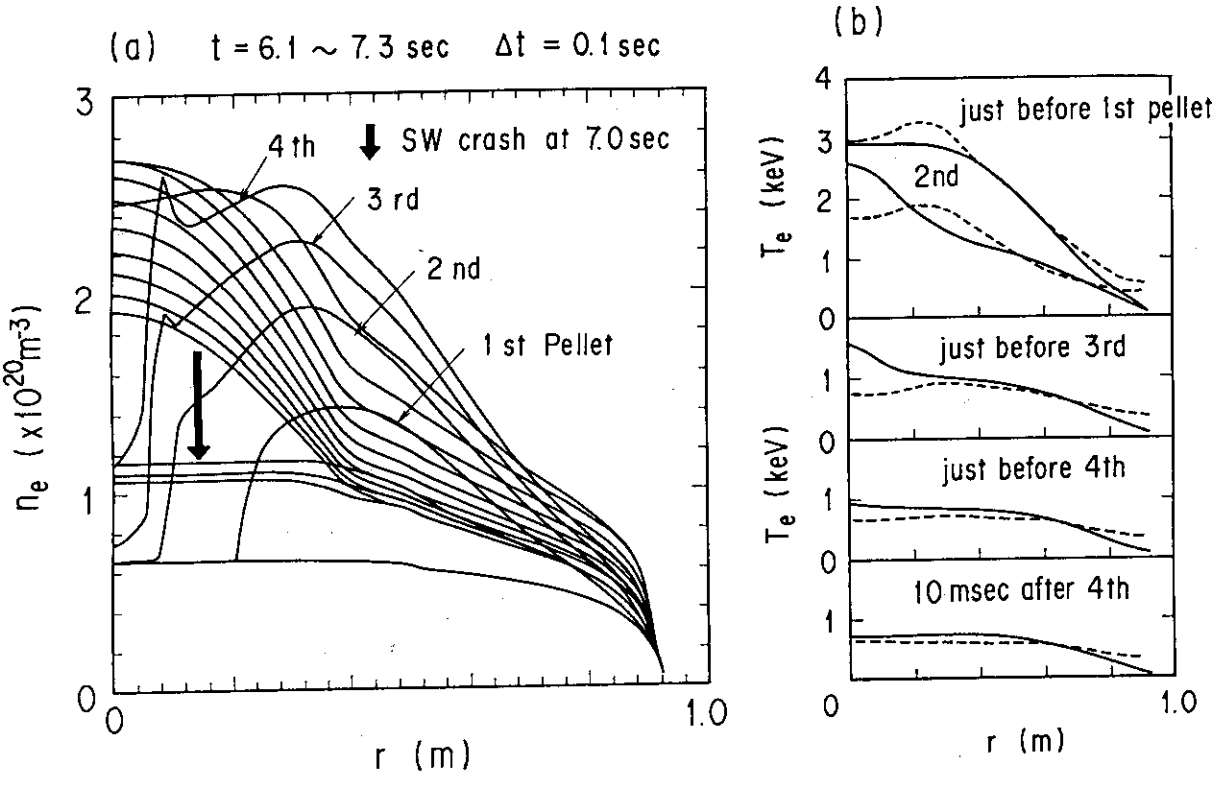


Fig. 5 (a) Pellet ablation profiles and relaxation of density profile after pellet injection in simulation for the shot E10814.

(b) Comparison of electron temperature profile between simulation result ( solid lines ) and measurement by soft X-ray Filter absorption method ( broken lines ).

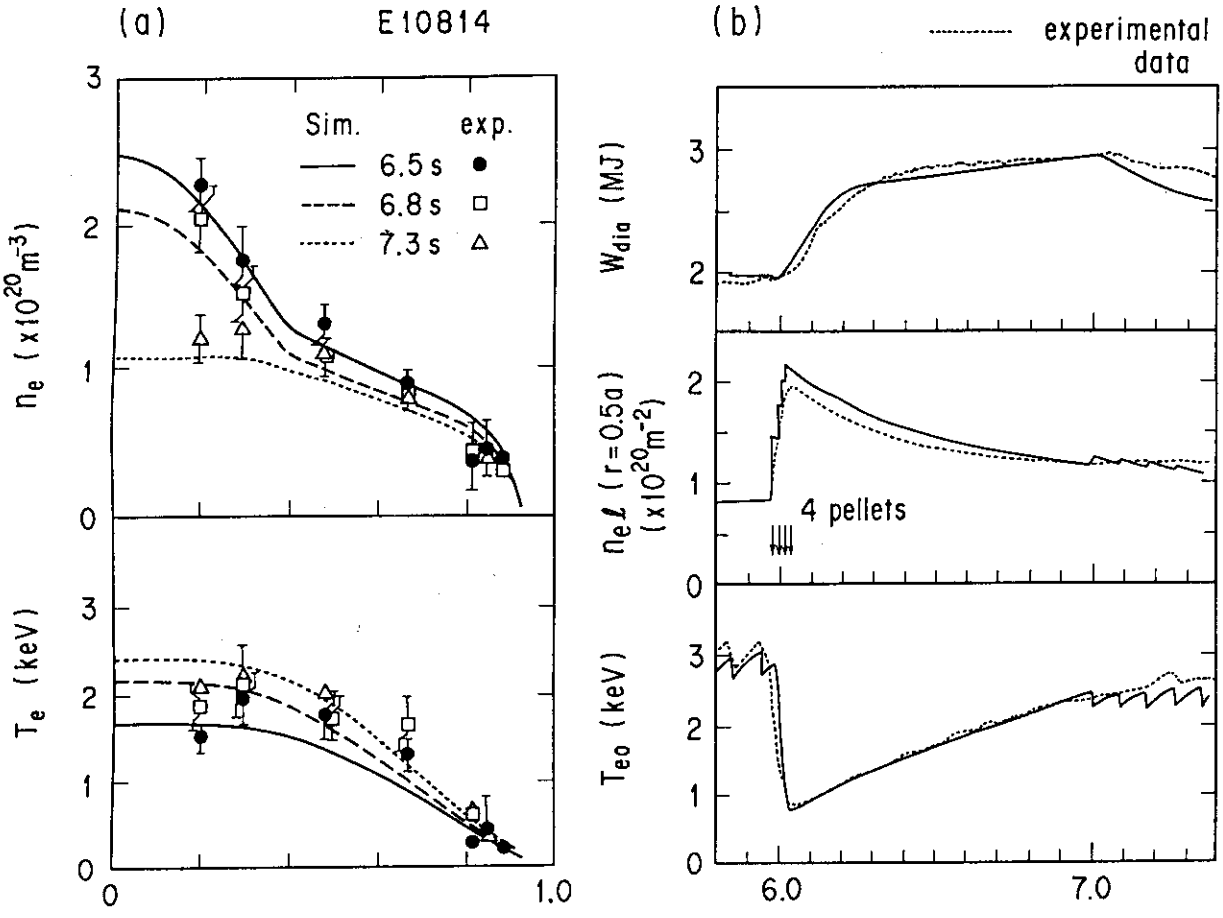


Fig. 6 Simulation result for the shot E10814 ( $I_p$ = 3.1 MA, $B_t$ = 4.5 T, $P_{NB}$ = 14 MW ) .

(a) Electron density and electron temperature profiles ( $n_e$ (r) and $T_e$ (r) ) . The profiles are in good agreement with measurement (Thomson data ) within the error bars.

(b) Time evolution of the stored energy ( $W_{ST}$ ) , the-line integrated density ( $\int n_e$ dl ) at r = 0.5 a and the electron temperature at the plasma center ( $T_{e0}$ ) . These results also agrees with the experimental data ( dotted lines ).

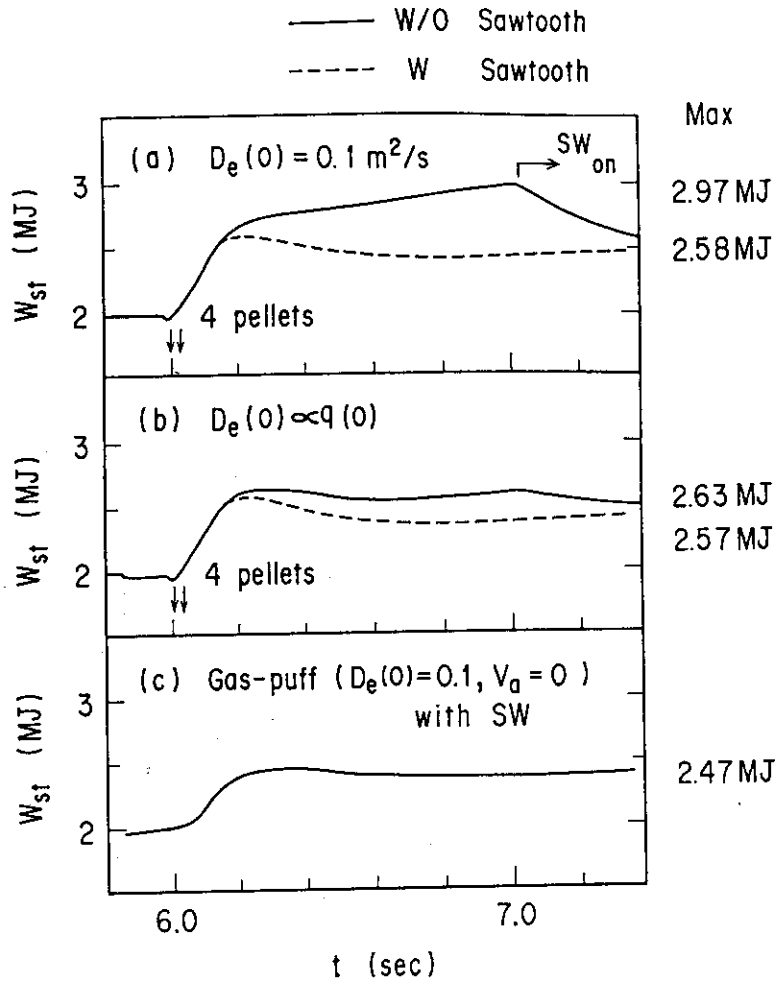


Fig. 7 Effect of sawtooth suppression on plasma stored energy

(a) : pellet fuelled plasma with the particle diffusivity reduced inside the q = 1 surface ( $D_e = 0.1\ m^2/s$ ) and the particle inward pinch ( $V_a = 0.4$ m/s ) .

(b) : pellet fuelled plasma with no good particle confinement inside $r_s$ ( $D_e \propto q(r)$ ) and the particle inward pinch.

(c) : gas fuelled plasma with good particle confinement inside $r_s$ ( $D_e = 0.1\ m^2/s$ ) , no inward pinch and sawtooth activity.

In case of (a) and (b), solid lines represent the stored energy of the plasma in which the sawtooth is suppressed till 7 sec and broken lines represent that including the sawtooth activity with $\tau_{SW} = 90$ msec..

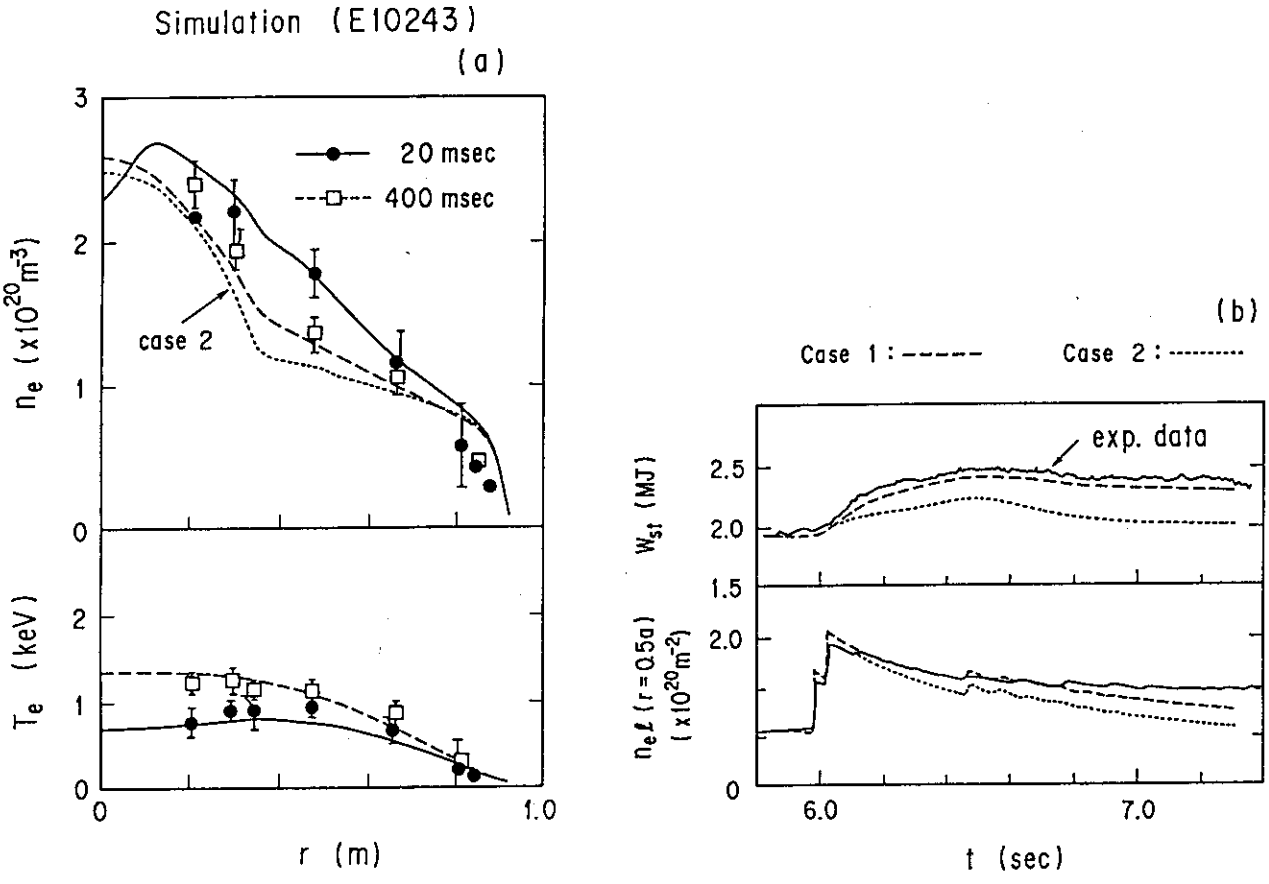


Fig. 8 Simulation result for the shot E10243 ( $I_p$ = 2.8 MA, $B_t$ = 4.5 T, $P_{NB}$ = 8 MW )

The calculation conditions of case 1 and 2 are as follows;

$V_a$ = 0.5 m/s, $D_e(q \leq 1)$ = 0.1 m$^2$/s and $V_a$ = 0.0 m/s, $D_e(q \leq 1)$ = 0.03 m$^2$/s ,

respectively.

(a) Profiles of electron density and temperature.

(b) Time evolution of the stored energy ( $W_{ST}$ ) and the line-integrated density ( $\int n_e \, dl$ ) at r = 0.5 a. Solid lines represent the experimental data.

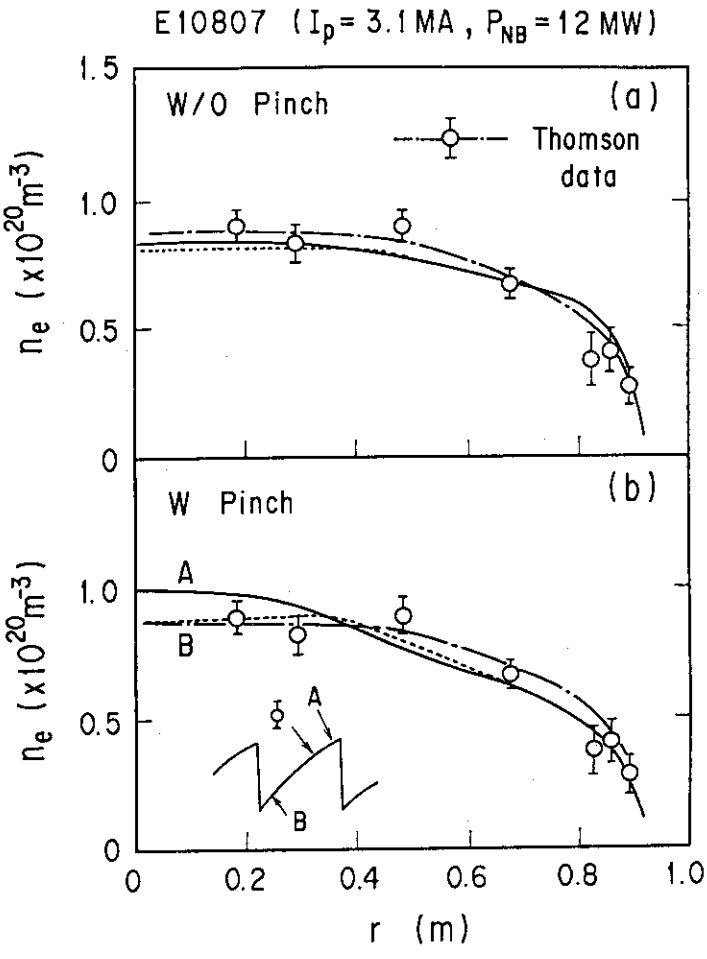


Fig. 9 Effect of inward pinch in gas fuelled plasma of shot E10807

( $I_p$ = 3.1 MA, $B_T$ = 4.5 T, $P_{NB}$ = 12 MW )

(a) : without , (b) : with inward pinch of $V_a$ = 0.4 m/s .

Solid lines (A) and dotted lines (B) represent the calculated density profiles before and after sawtooth crash, respectively. Dot-broken lines represents the experimental data ( Thomson data ).

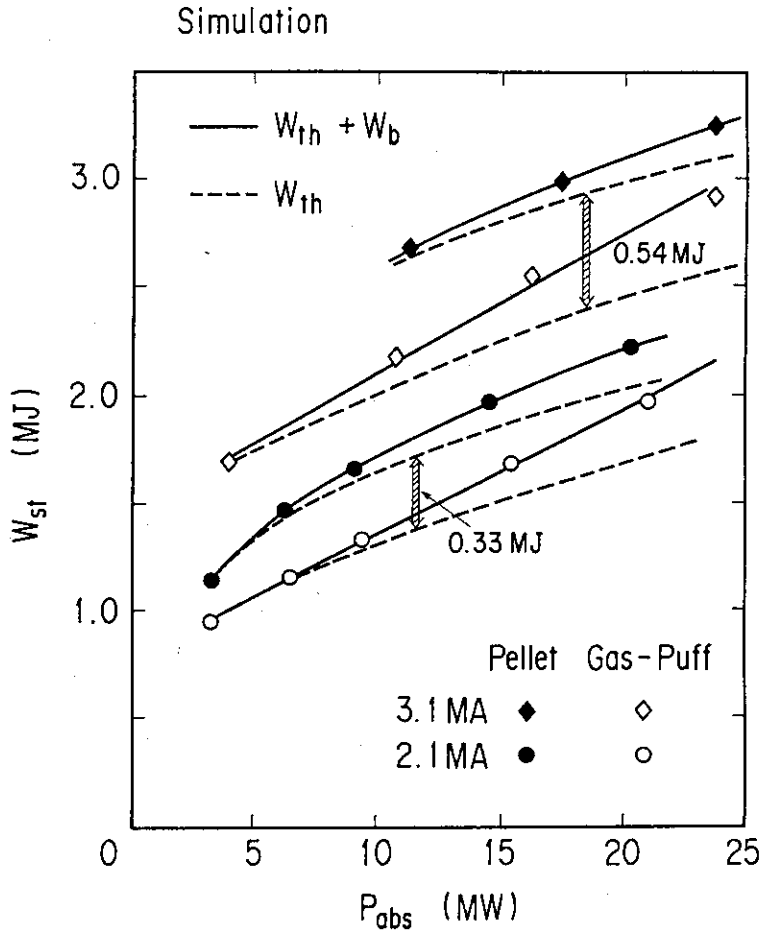


Fig. 10 Power dependence of the stored energy obtained in simulations.

The simulations are carried out for pellet fuelled plasmas ( closed symbols ) under the condition of the well center peaked ablation profiles and the sawtooth suppression during 1 sec after pellet injection.

Solid lines and broken lines represent the stored energy including the beam component and the thermal stored energy, respectively.

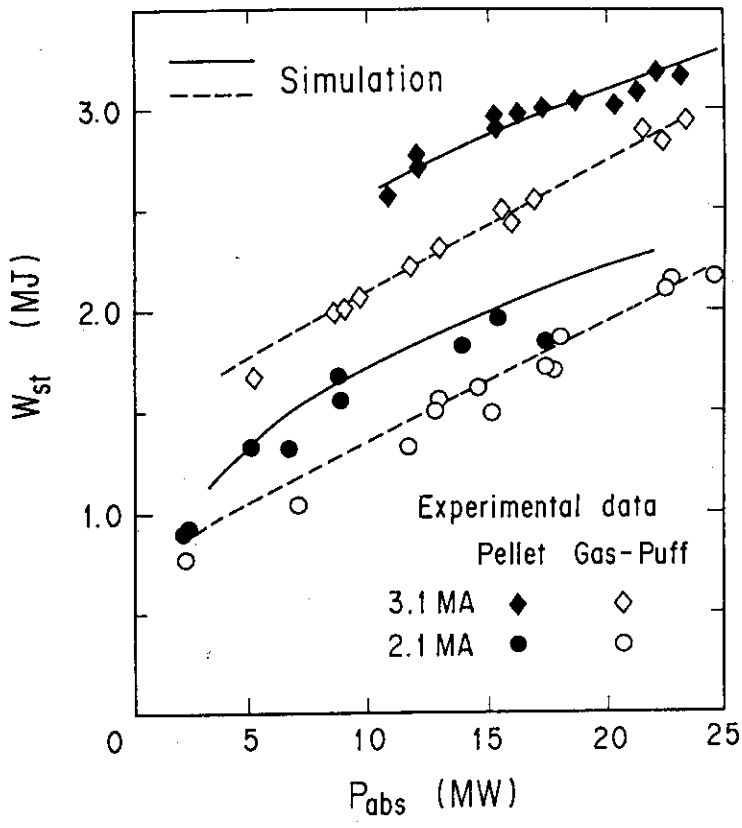


Fig. 11 Comparison of stored energy with experimental data.

Solid lines and broken lines represent the simulation result for the pellet and gas fuelled plasmas, respectively. The symbols represent the experimental data. These meanings are the same of those in Fig. 1.

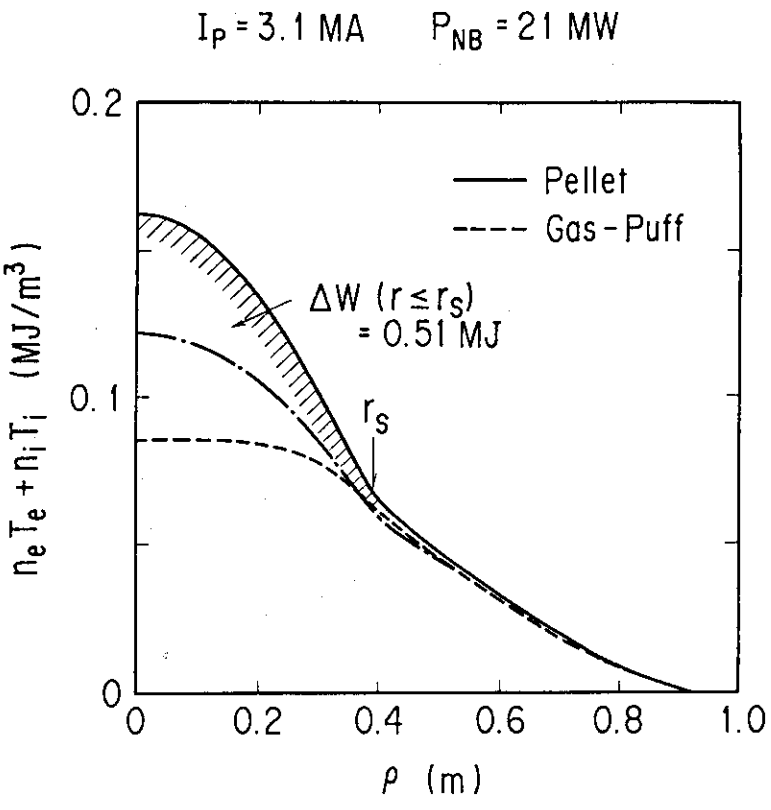


Fig. 12 The pressure profiles for 3.1 MA plasma with NBI heating power of 21 MW. The solid line and the broken line represent the pressure profile for the pellet and gas fuelled plasma, respectively. The improvement in the stored energy is due to the peaked pressure profile inside the q = 1 surface. The pressure profile for the pellet fuelled plasma without the inward pinch is shown by the broken line.

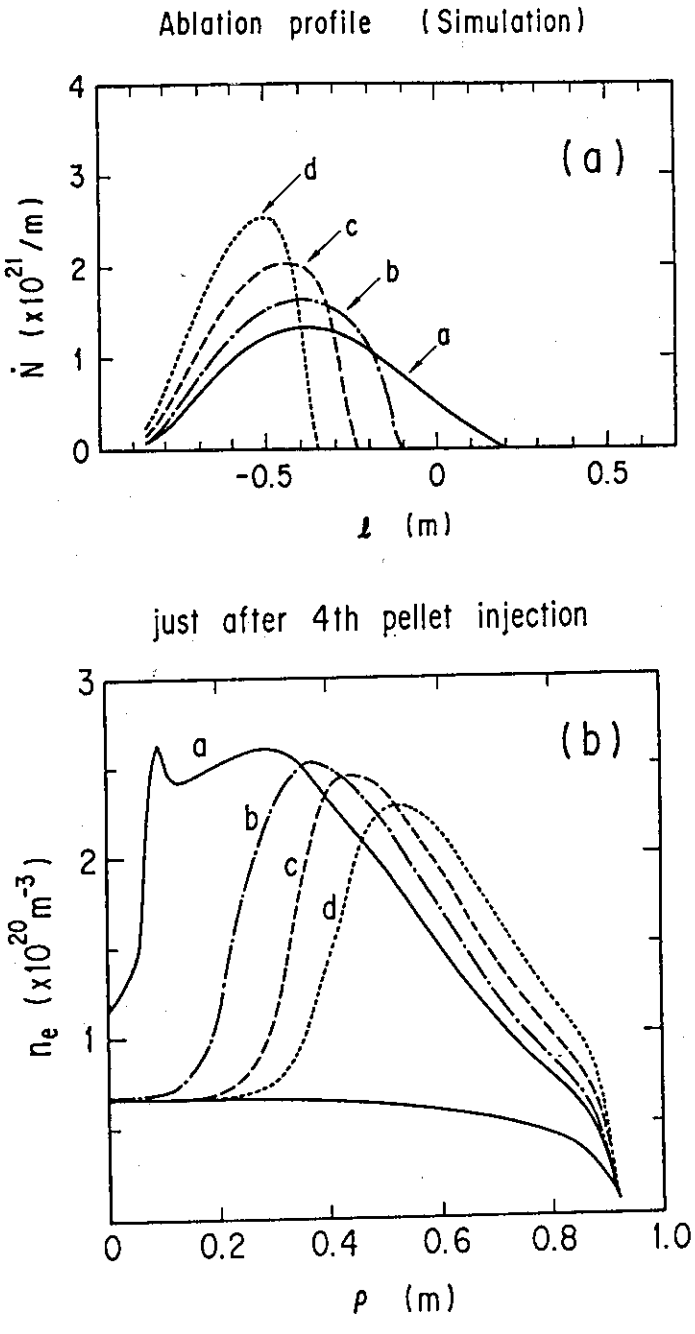


Fig. 13 (a) Ablation profiles along pellet path length.

These profiles are used in the simulations of subsection 4.4.

(b) Density profiles just after pellet injection.

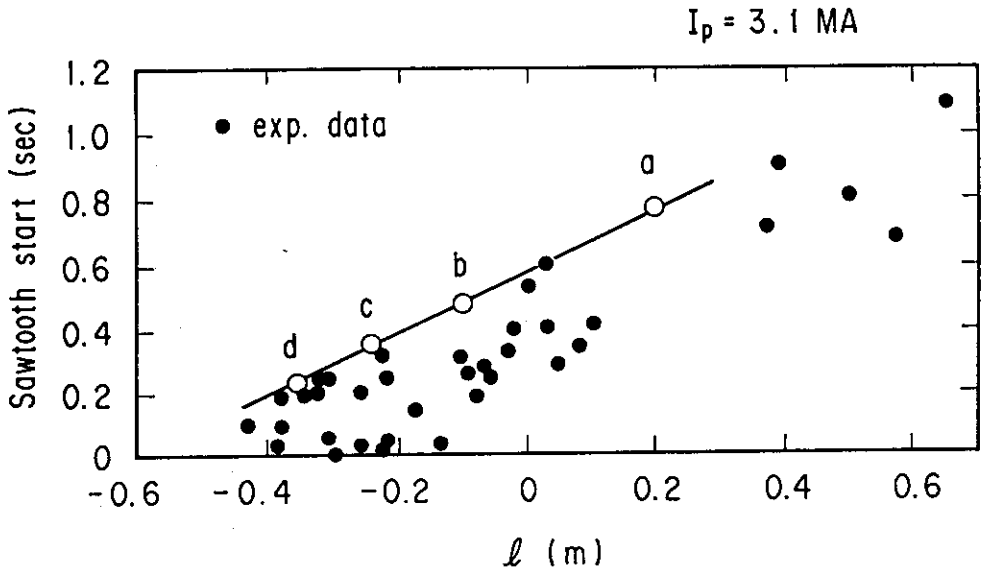


Fig. 14 Relationship between penetration depth and sawtooth start time after pellet injection ( experimental result ). The sawtooth start time in the simulation is determined from the relation shown by the solid line, which is based on the experimental data. For the ablation profiles of (a), (b), (c) and (d) in Fig. 13 (a), sawtooth is supposed to start at 0.75 sec, 0.40 sec, 0.35 sec and 0.20 sec after the pellet injection, respectively.

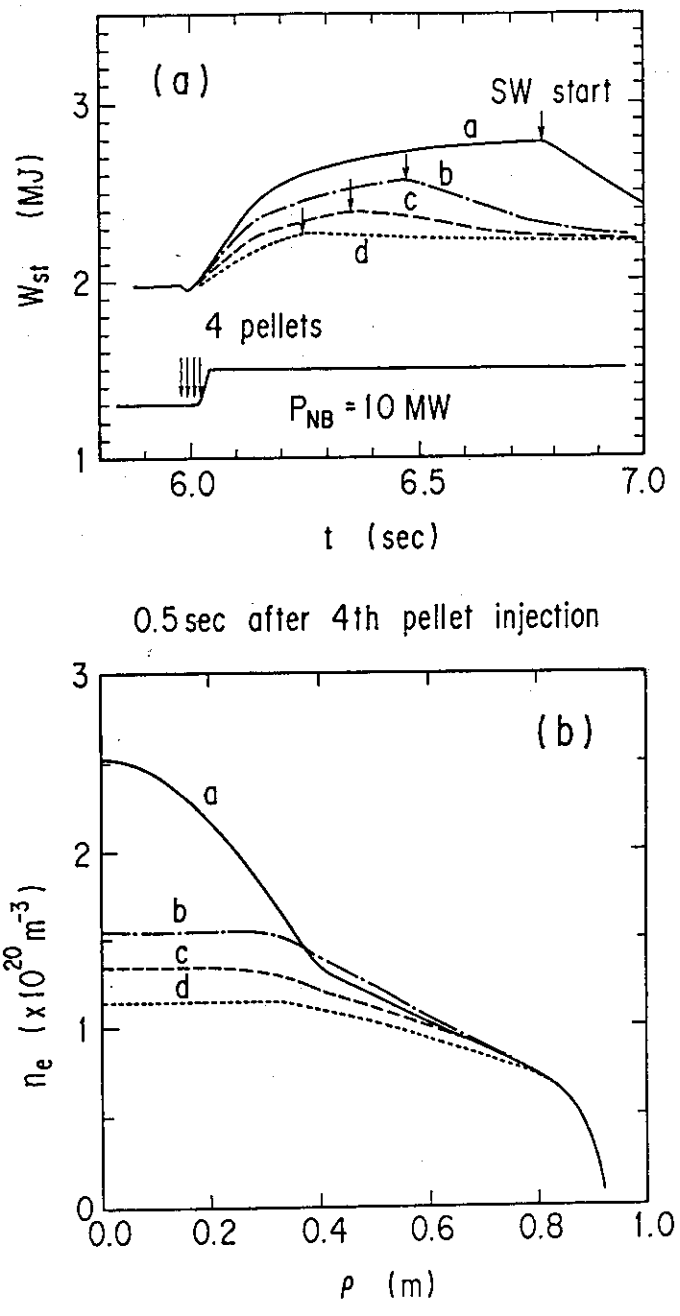


Fig. 15 (a) Time evolution of stored energy. The stored energy starts to decrease after the sawtooth crash indicated by the arrows. The inward pinch is terminated after the sawtooth crash.

(b) Density profiles at 0.5 sec after pellet injection.

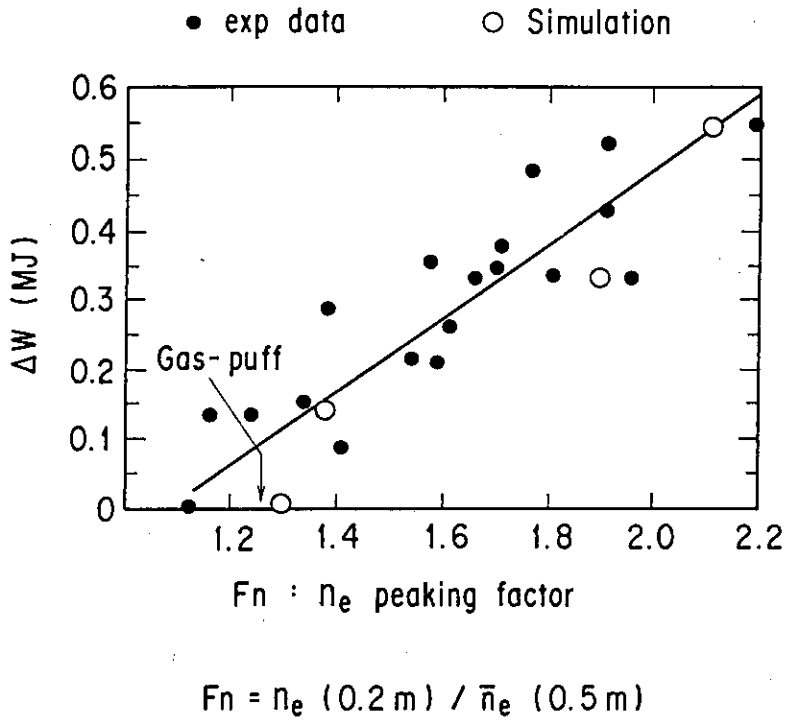


Fig. 16 Relation between density peaking factor ( $F_n$ ) and improvement in stored energy ( $\Delta W$ ). The peaking factor is defined by the ratio of the off-axial line averaged density and the density at r = 0.2 a which is the inmost measurable position of the Thomson scattering system. Open symbols are the relation between $F_n$ and $\Delta W$ obtained from the simulation result in Fig. 14 and closed symbols are experimental data.

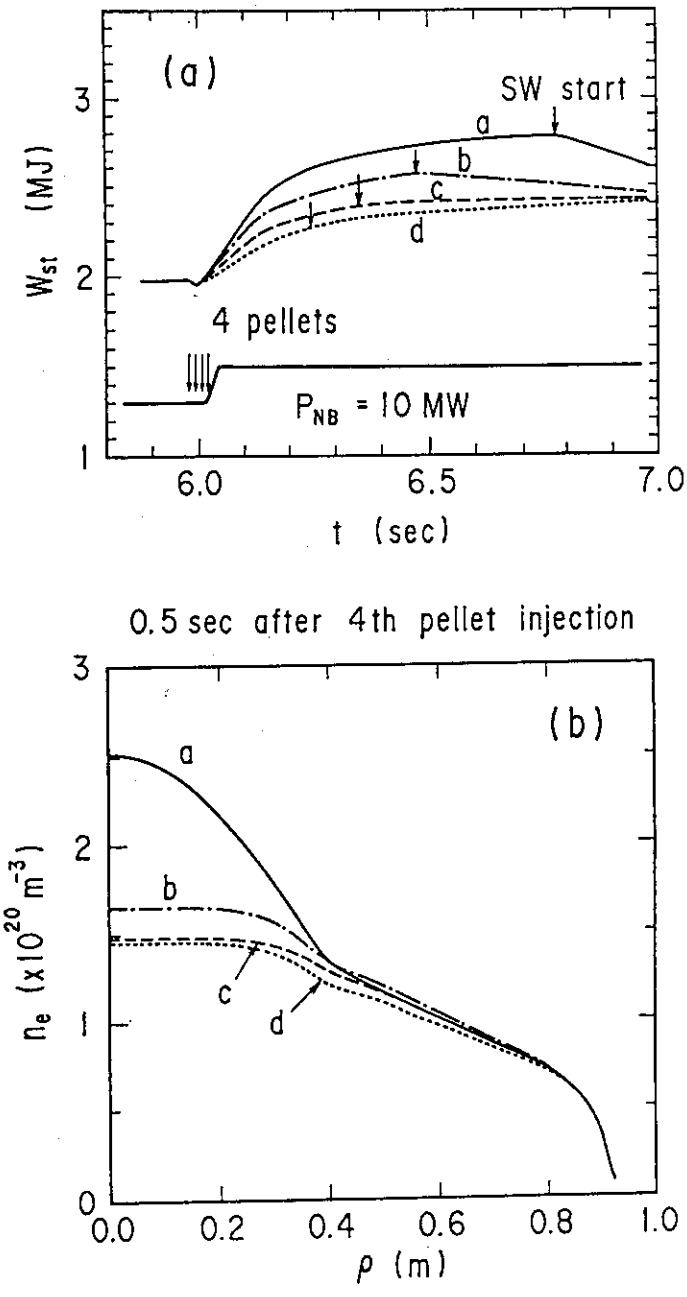


Fig. 17 (a) Time evolution of stored energy. The inward pinch is not terminated after the sawtooth crash in contrast to the simulation in Fig. 14. The stored energy continue to increase after the sawtooth crash by the effect of the inward pinch in the case of c and d.

(b) Density profiles at 0.5 sec after pellet injection.

## Appendix A Effect of Reduction in Thermal Diffusivity

The effect of the reduction in thermal diffusivity within the q = 1 surface on the electron temperature is presented in this Appendix. Figure A-1 (a) shows the spatial dependence of the diffusion coefficients of $D_e$ , $\chi_e$ and $\chi_i$ and Fig. A-1 (b) shows the calculated electron temperature profiles before (solid lines) and after (broken lines) the sawtooth crash. When the $\chi_e$ and $\chi_i$ within $r_s$ is improved by a factor of ~ 2.5, the amplitude of electron temperature change $\Delta T_{e0}$ is about 600 eV, whereas in the experiment $\Delta T_{e0}$ is 300 ~ 400 eV. By using the empirical L-mode diffusion coefficient used in our simulations can be well reproduced. The effect of the good energy confinement can not be masked by the sawtooth oscillation, in contrast to the good particle confinement within $r_s$ , because the heat source is applied in the central region.

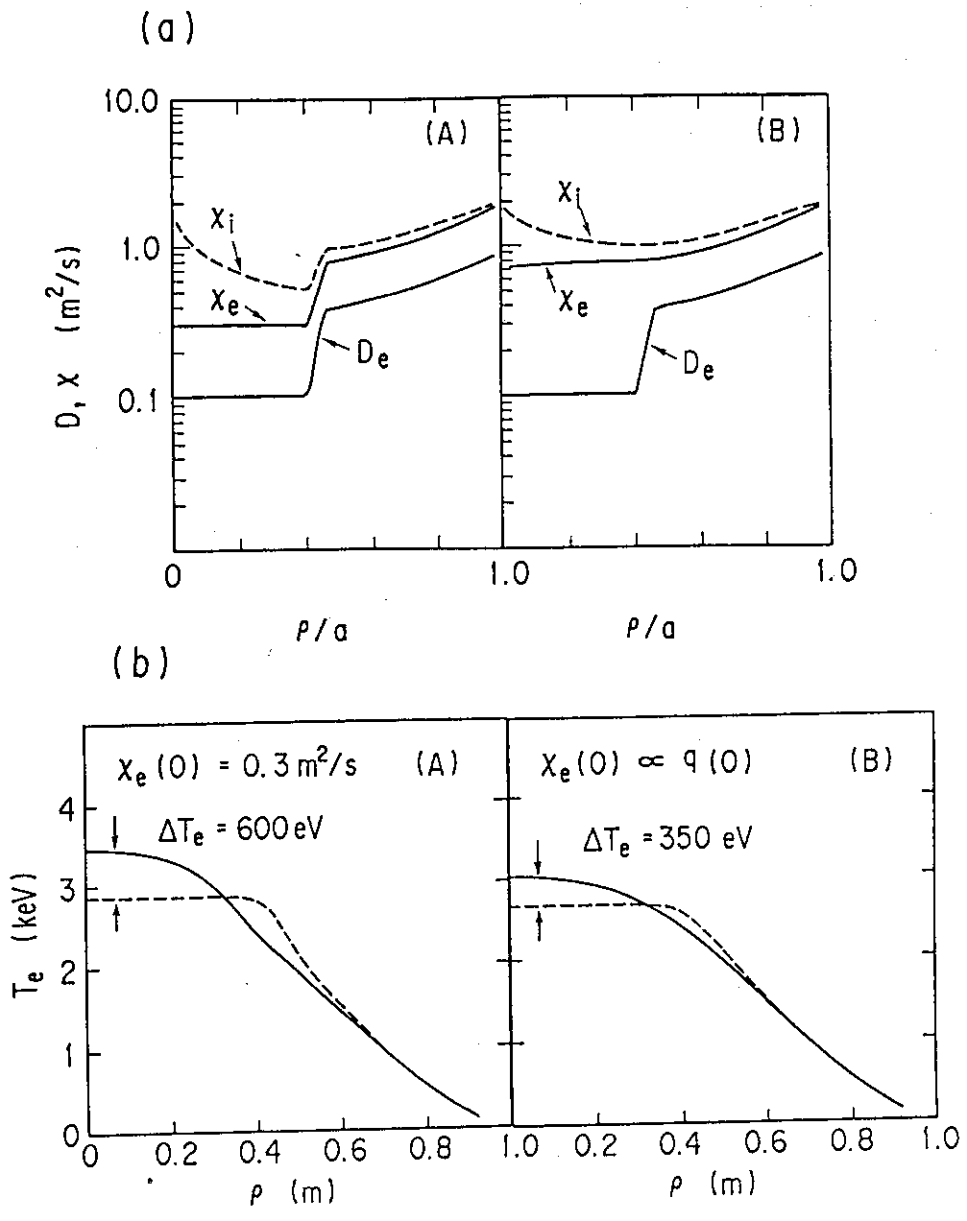


Fig. A-1 Effect of reduction in thermal diffusivity within the q = 1 surface.

(a) Spatial dependence of diffusion coefficients of $D_e$ , $\chi_e$ and $\chi_i$ .

(b) Calculated electron temperature profiles.

Solid lines and broken lines present Te (r) before and after sawtooth crash, respectively.

## Appendix B Correlation between Penetration Depth and Sawtooth Suppression

We propose the new model of sawtooth based on the experimental fact. The q = 1 position $r_s$ at the sawtooth crash is almost unchanged for Ohmic plasma and neutral beam heated plasma with the same same safety factor at the plasma surface [ 6 ]. We employ the criterion that a sawtooth crash takes place at the moment when the q = 1 position reaches to 1.1 a / q(a) . The sawtooth period is determined automatically in this model. The simulation result for neutral beam heated plasma is shown in Fig. B-1. The sawtooth period of 105 msec is obtained and it agrees with the experimental data. This result indicates that the criterion for timing of sawtooth crash is quite reasonable. Figure B-2 shows the relaxation of the density profile $n_e$ (r), the electron temperature profile $T_e$ (r) and the current density profile $J_z$ (r) for the well center peaked ablation case (a) and the shallow ablation case (b). In the shallow ablation case, the high electron temperature in the central region is kept and it follows that the density profile becomes shrink. The q = 1 singular surface moves outwards and the sawtooth crash takes place at the early phase after the pellet injection. On the other hand, in the center peaked ablation, the increase of the current density at the center is suppressed by the low electron temperature. The q = 1 surface dose not move outward and the sawtooth crash is prolonged up to 0.6 sec. The relation between the penetration depth of the pellet and the sawtooth suppression obtained from simulations is shown by open squares in Fig. B-3. The result is consistent with the experimental data. The correlation between the penetration length of pellet and the sawtooth suppression can be explained by the shrink of the current channel.

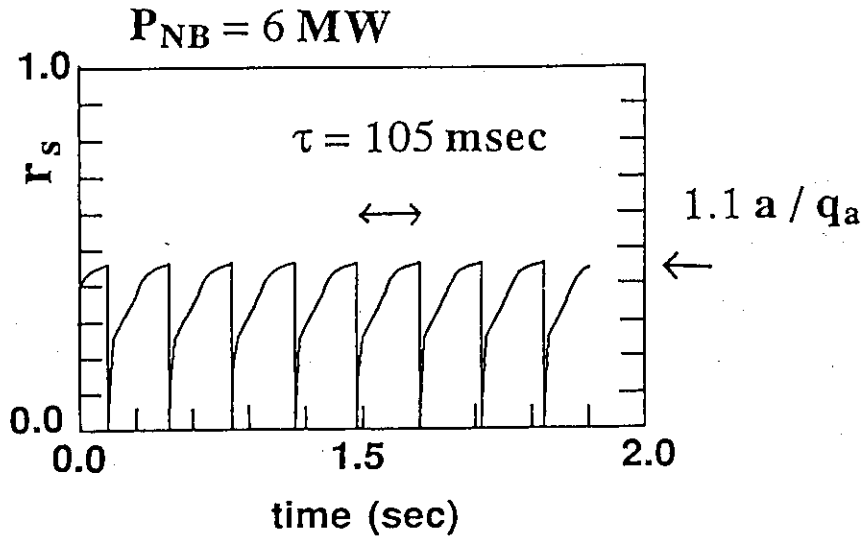


Fig. B-1 Time evolution of q = 1 position

Sawtooth period is 105 msec which is consistent with the experimental data of 90 ~ 150 msec.

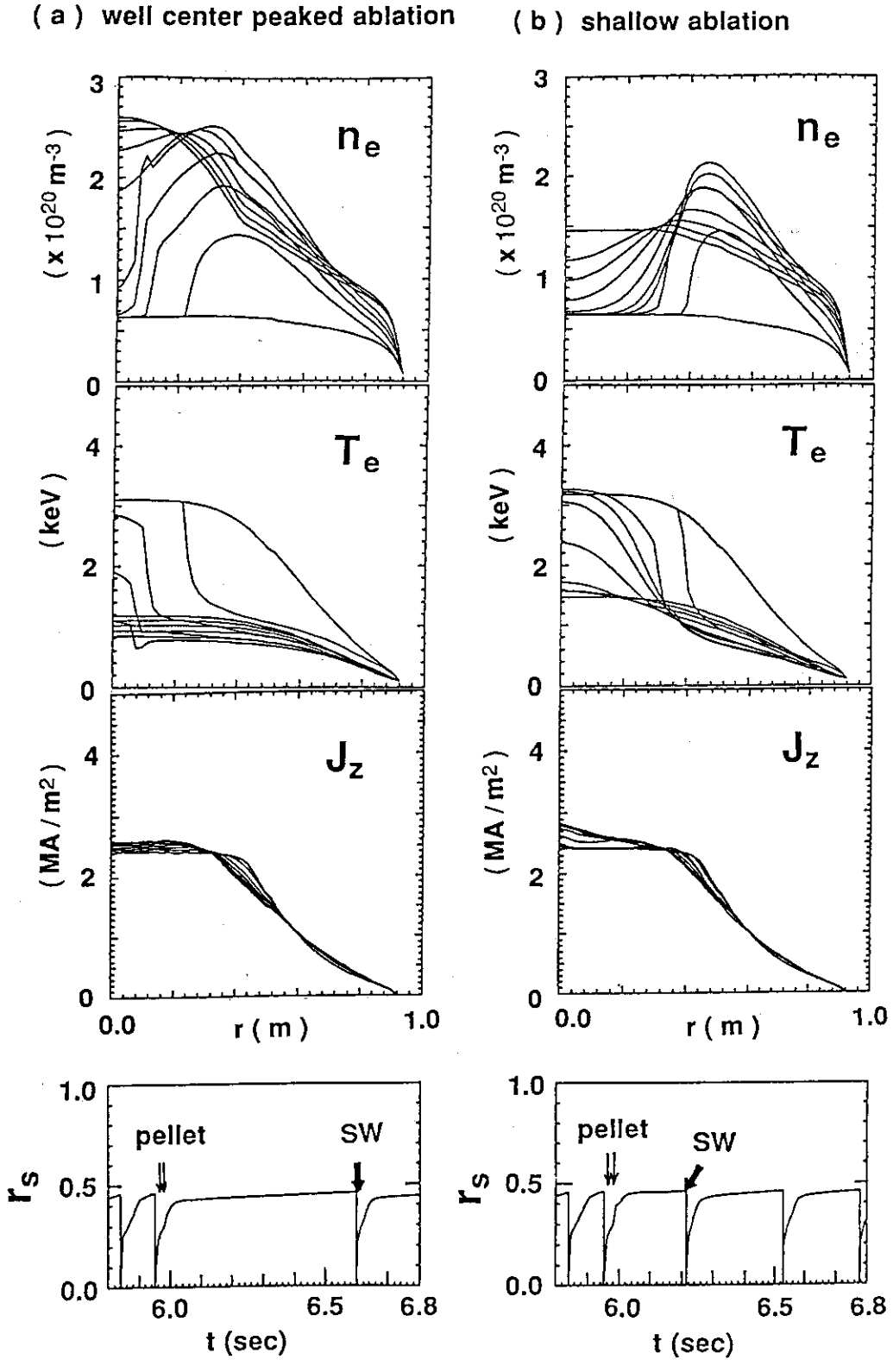


Fig. B-2 Relaxation of the density profile $n_e$ (r), the electron temperature profile $T_e$ (r) and the current density profile $J_z$ (r) after pellet injection and time evolution of q =1 surface. The well center peaked ablation profile and the shallow ablation profiles are used in case (a) and (b), respectively.

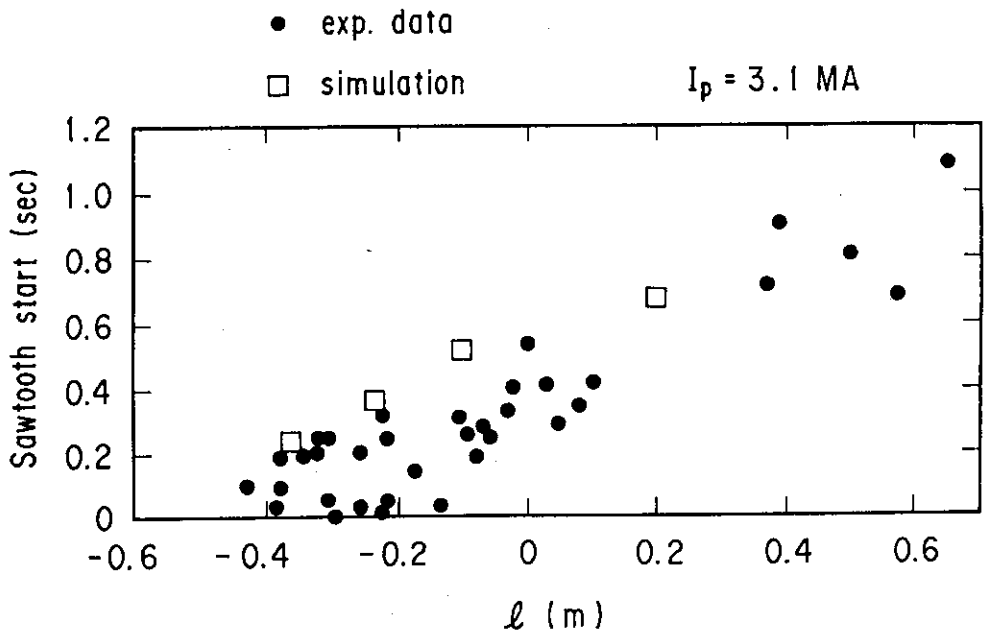


Fig. B-3 Relation between the penetration depth of the pellet and the sawtooth suppression. Closed circles and open squares denote the experimental data and simulation results, respectively.